Journal of Applied Research and Technology

www.jart.ccadet.unam.mx
Journal of Applied Research and Technology 16 (2018) 484-497

Original

Influence of incorporating a small amount of silica on the catalytic performance of a MoO_3/Al_2O_3 catalyst in ethanol oxidative dehydrogenation

Aline Villarreal [a, b], Gabriella Garbarino [a, d], Paola Riani [c, d], Aida Gutiérrez-Alejandre [b,*], Jorge Ramírez [b], Guido Busca [a, d]

[a] *Dipartimento di Ingegneria Civile, Chimica e Ambientale (DICCA), Università degli Studi di Genova, Piazzale Kennedy, 1, I-16129 Genoa, Italy*

[b] *UNICAT, Departamento de Ingeniería Química, Facultad de Química, Universidad Nacional Autónoma de México (UNAM), Ciudad de México, CP 04510, Mexico*

[c] *Dipartimento di Chimica e Chimica Industriale (DCCI), Università degli Studi di Genova, Via Dodecaneso, 31, I-16146 Genoa, Italy*

[d] *INSTM, UdR di Genova, Via Dodecaneso, 31, I-16146 Genoa Italy*

Abstract: The influence of incorporating a small amount of silica on the catalytic performance of MoO_3/Al_2O_3 catalyst was studied. Molybdenum supported on pure alumina and 5% SiO_2-Al_2O_3 supports were synthesized. The catalysts were characterized by XRD, Raman, UV-Vis and IR spectroscopies, FE-SEM microscopy, and their activity was evaluated in the oxidative dehydrogenation of ethanol to acetaldehyde. Molybdenum supported on pure alumina gives a 74% yield to acetaldehyde (at 573 K) due to the generation of oxy-dehydrogenation active sites by molybdenum and to the decrement of the alumina dehydration sites. For the molybdenum catalyst supported on silica-containing alumina, the molybdenum species were displaced from the strongest alumina's acid-base couples, located on nanoparticles edges, corners and defects, to weaker ones located on plane faces causing the rise of weakly bonded species with less active redox behavior.

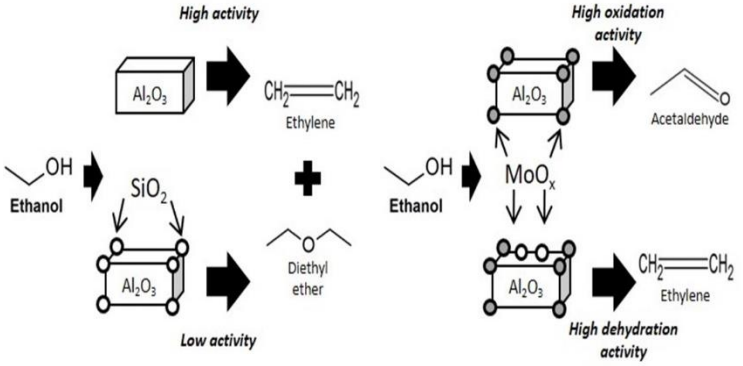

Keywords: Molybdenum oxide catalysts; alumina support; dispersion of Mo oxide catalysts; acetaldehyde production; ethanol oxy-dehydrogenation

* Corresponding author.
E-mail address: aidag@unam.mx (Aida Gutiérrez-Alejandre).
Peer Review under the responsibility of Universidad Nacional Autónoma de México.

1. INTRODUCTION

Bioethanol produced from non-food biomass is called second generation bioethanol and it is expected to become a very relevant intermediate or platform compound in the future, when renewables (mostly lignocellulosics) will represent the raw materials to yield value chemicals and (bio) fuels. Bioethanol gives great opportunities to produce a broad variety of high-added value chemicals such as diethyl ether, ethylene, acetaldehyde, acetic acid, propylene which is the second most important building block chemical in petrochemical industry after ethylene and aromatics.

The transition alumina phase, γ-Al_2O_3, is a very important material used as adsorbent, catalyst and support in the petroleum and chemical industries (Busca, 2014). Alumina is widely used as support of numerous metallic, oxide and sulfide industrial catalysts. Recently, molybdenum catalysts supported on alumina (~12 wt%, ~200 m^2/g)) have been used in the conversion of ethanol to acetaldehyde. (Balat, 2011; Limayem & Ricke, 2012). (Bio)ethylene (Mohsenzadeh, Zamani, & Taherzadeh, 2017) and diethyl ether can be obtained by the catalytic bio(ethanol) dehydration, typically obtained over acidic catalysts such as γ-Al_2O_3 (Phung, Proietti Hernández, Lagazzo, & Busca, 2015), while acetaldehyde can be the primary product of ethanol dehydrogenation or oxidative dehydrogenation. Pure and oxidative ethanol dehydrogenation processes have been applied industrially in early times to produce acetaldehyde from ethanol over copper and silver catalysts, with high (but not complete) selectivity only at low conversions, thus with the recycling of unreacted ethanol (Chauvel & Lefebvre, 1989; Eckert, Fleischmann, Jira, Hermann, & Golka, 2006; Weissermel & Arpe, 2003) in detriment of the process economy.

In addition of interesting catalytic activity for several reactions (Akbari, Omidkhah, & Towfighi, 2014; Haddad, Bordes-Richard, Hilaire, & Barama, 2007; Marakatti, Mumbaraddi, Shanbhag, Halgeri, & Maradur, 2015; Noureddini & Kanabur, 1999; Peeters et al., 1998; Sankaranarayanan, Pandurangan, Banu, & Sivasanker, 2011; Sheldon & Van Bekkum, 2002; Teimouri, Najari, Najafi Chermahini, Salavati, & Fazel-Najafabadi, 2014), most of the interest for MoO_3/γ-Al_2O_3 materials is due to their role as precursors of Ni- or Co- promoted MoS_2/γ-Al_2O_3 catalysts for hydrotreatment processes (Toulhoat & Pascal, 2013). For these catalysts, the interaction of the molybdenum oxide species with the support is critical, determining the extent and easiness of the subsequent active species genesis, the distribution and dispersion of the promoters (Ni and Co), and in consequence their final activity. It has been shown, that the addition of silica affects the nature of the molybdena-alumina interaction allowing a more extensive active phase formation (sulfidation) (Ramirez & Sánchez-Minero, 2008), (Sánchez-Minero, Ramírez, Cuevas-García, Gutiérrez-Alejandre, & Fernández-Vargas, 2009).

The aim of this work is to study the activity and selectivity of MoO_3/γ-Al_2O_3 catalysts in ethanol oxidative dehydrogenation as model reaction, to probe the interaction of MoO_3 and SiO_2 with the alumina surface to assist in the synthesis of high active catalysts for oxidation and hydrotreating reactions. We analyzed in detail, using a variety of characterization techniques (FTIR, Raman, UV-VIS, XRD and FE-SEM/EDX microscopy), how the presence of a small amount of silica (5 wt % SiO_2) in the alumina support changes the molybdena/alumina interaction, affects the chemistry of the support surface and the nature of the Mo supported species.

2. MATERIAL AND METHODS

2.1 CATALYST PREPARATION

The catalyst supports were Puralox Sba 200 (γ-Al_2O_3), and Siralox 5/170 (γ- Al_2O_3 with 5 wt% SiO_2), hereinafter denoted as A and SA, both produced by Sasol. Supported molybdena catalysts with 11.9 wt.% MoO_3 (wt $_{MoO3}$/wt $_{support}$) were prepared by wet impregnation using an aqueous solution of $(NH_4)_6Mo_7O_{24}$*$4H_2O$ (Aldrich, 99%). The samples were stirred five hours at 363 K until dry, and then calcined in air at 773 K for 5 h.

2.2 CATALYTIC CHARACTERIZATION

XRD analyses of the fresh catalysts were performed on a X'Pert diffractometer (CuKα radiation, Ni filter; operated in the vertical mode at 40 kV and 30 mA). The patterns were recorded over the 2θ angle ranging from 10° to 100° with a step of 0.02° and a counting time for each step of at least 11 s. Powder patterns were indexed by comparing experimental results to the data reported in the Pearson's Crystal Data database.

Raman spectra were collected in a ThermoScientific Micro-Raman spectrophotometer at ambient conditions. Spectra have been collected with 100 scans and a resolution of 4 cm^{-1}.

DR-UV-Vis-NIR spectra of both fresh and spent catalysts were collected with a JASCO V570 instrument equipped with an integrating sphere.

Qualitative and quantitative analyses were carried out by using a scanning electron microscope (SEM) Zeiss Evo 40 equipped with a Pentafet Link Energy Dispersive X-ray Spectroscopy (EDXS) system managed by the INCA Energy software (Oxford Instruments). For qualitative and quantitative analyses, the samples were analyzed employing an acceleration voltage of 20 kV, using a Co standard for calibration in order to monitor beam current, gain, and resolution of the spectrometer.

A Zeiss SUPRA 40 VP Scanning Electron Microscope, equipped with a field emission gun was used to investigate sample morphology. This instrument (FE-SEM) is equipped with a high sensitivity "InLens" secondary electron detector and with an OXFORD "INCA Energie 450x3". Sample powders were directly mounted on a high purity conductive double sided adhesive carbon tabs or were suspended in ethanol under ultrasonic vibrations to decrease particle aggregation, then a drop of the resultant mixture was deposited on a copper tape and the dried sample was then imaged.

IR spectra were recorded using Nicolet 380 FT-IR spectrometer. For skeletal studies, the samples were pressed into thin wafers with KBr (1:100 dilution) and spectra were recorded at room conditions air. Spectra have been collected with 100 scans and a resolution of 2 cm^{-1}.
For surface characterization by IR analysis, pure powder pressed disks (20-30 mg) were activated in vacuum at 773 K in the IR cell ('activated surface') for one hour, then cooled down to room temperature, and contacted with 35 torr of spectroscopically pure CO_2 (from SIAD). The spectra of surface species were recorded in the presence of CO_2 gas at two different partial pressures, after outgassing at room temperature and upon outgassing till 673 K.

The catalytic experiments were performed at atmospheric pressure in a tubular flow reactor (i.d. 7 mm) using 0.50 g of catalyst (60-70 mesh, thus achieving a ratio between the particle and internal reactor diameter near 25) and feeding ethanol (96% assay, from Sigma Aldrich) in nitrogen with a total flow rate of 80 cc/min. For oxidation tests, the following gas composition and parameters have been used: 2.1% C_2H_6O, 14.8% O_2, 83.1% N_2 total flow 80 cc/min, catalyst weight 0.50 g. The carrier gas (N_2) was passed through a bubbler containing ethanol maintained at constant temperature (298 K) to obtain the desired partial pressures. The temperature in the experiment was varied stepwise from 423 K to 773 K. In Figure 1 is showed the experimental set-up for testing catalytic performance.
Outlet gas analyses were performed with an Agilent 4890 gas chromatograph (GC) equipped with a Varian "Molsieve 5A / Porabond Q Tandem" capillary column and TCD and FID detectors in series. Thermo Scientific GC-MS with TG-SQC column (30 m L x 0.25 mm ID x 0.25 μm thick) was used for qualitative/quantitative analyses. The injected volume for each analysis was 50 μl. From the peak areas, the concentrations have been obtained and then the molar flow rates have been evaluated. Ethanol conversion and selectivities to products (1) and (2), respectively, are defined as follows:

$$X_{EtOH} = (n_{EtOH(in)} - n_{EtOH(out)})/n_{EtOH(in)} \quad (1)$$

$$S_i = n_i/(\nu_i(n_{EtOH(in)} - n_{EtOH(out)})) \quad (2)$$

where n_i = moles of compound i, and ν_i = ratio of stoichiometric reaction coefficients. The mass balance is essentially always fulfilled in these experiments. Repeated experiments show that uncertainty in the measures is near ~5%.

3. RESULTS

3.1 STRUCTURAL CATALYST CHARACTERIZATION

XRD results show that sample A is cubic γ-Al_2O_3 while SA has the pattern of the more distorted structure of δ-Al_2O_3, see Fig. 2 (Busca, 2014; Hillerová, Morishige, Inamura, & Zdražil, 1997). This is confirmed by skeletal IR (Fig. 3, left) that shows the typical broad and large features of γ-Al_2O_3 in the case of sample A, and the more complex and sharper features of the more distorted structure of δ-Al_2O_3 for sample SA. Additionally, a quite broad absorption with maximum near 1040 cm^{-1} is found on SA (evidenced in the subtraction SA-A, Fig. 3, right) due to Si-O stretching modes of silicate species, which is cut at lower frequencies by the negative band at 935 cm^{-1}, associated to the perturbation of Al-O modes due to silica deposition (Finocchio et al., 1997). These features show that silicon species on SA are in the form of isolated silicate species, deposed on aluminum oxide surface sites. Polymeric silicate species cannot be observed.

The diffraction patterns of the molybdenum-containing samples do not show additional peaks besides those of the supports (Fig. 2). The characteristic peaks associated to molybdenum oxides have been not observed.

Subtracted skeletal IR spectra of both MoA and MoSA (i.e. the MoA-A and MoSA-SA subtractions, Fig. 3, right) show a band near 948 cm^{-1}, assigned to Mo=O stretchings of molybdenyl bonds. Also, the Raman spectra of both Mo-containing catalysts, MoA and MoSA (recorded in wet conditions, i.e. without performing drying procedures, Fig. 4), show a strong band near 950 cm^{-1}, assigned too to Mo=O stretchings of molybdenyl bonds.

3.2 SURFACE CATALYSTS CHARACTERIZATION BY IR SPECTROSCOPY

The IR spectrum of A outgassed at 773 K (Fig. 5) shows bands at 3790 (Al_{Th}-OH), 3767 (($\square$-O-Al_{Th}-OH), 3726 ($\square$-O-Al_{Oh}-OH) and 3685 cm^{-1} (Al-OH-Al), typical of the surface OHs of γ-Al_2O_3 (Busca, 2014; Hillerová et al., 1997). An additional sharp band at 3741 cm^{-1} (poorly split from the one at 3726 cm^{-1}), assigned to OH stretching of a silanol group, is observed in the spectrum of SA, while the component at 3767 cm^{-1} disappears and all others are strongly reduced in intensity except the one at 3790 cm^{-1}.

In Fig. 6, the spectra of the adsorbed species arising from CO_2 adsorbed on activated A and SA samples are reported. The most intense band that arises at 2345 cm^{-1} with shoulders at higher frequencies (2355 and 2365 cm^{-1}) is due to asymmetric stretching of CO_2 molecules adsorbed linearly on Lewis acid sites. Also, several bands from slightly different surface hydrogencarbonate species arise at 1646, 1485, 1442 and 1231 cm^{-1} due to ν_{asCOO}, ν_{sCOO} and δ_{OH} vibrational modes(split ν_{sCOO}) (Busca & Lavalley, 1986). This shows that over activated A, acid-basic sites exist converting CO_2 into hydrogencarbonate species. The bands of both CO_2 and hydrogencarbonate species are weaker in the spectrum of SA than in A, showing that silicate species (at least part of which are in the form of hydrogensilicate ions HO-SiO_3) "neutralize" in large part both, the strongest acid-base pairs and Lewis sites of the alumina surface. As discussed elsewhere (Busca, 2014), these sites are likely located on edges and corners of the alumina nanocrystals, thus this result let us to assume that silicate species depose primarily on edges and corners of alumina nanocrystals.

In the OH stretching region (Figure 5), the IR spectra of the MoA and MoSA, show a strongly decreased absorption with respect to the respective supports, with very weak residual bands due to Al-OH groups and Si-OH groups for MoSA. The total intensity in the region is even lower for MoSA than for MoA. This suggests that the effects of the addition of silicon and molybdenum to A on the Al-OH bands are similar, both species anchoring on the same alumina surface sites. The addition of molybdenum on SA further reduces the intensities of Al-OH bands, nearly completing the formation of a "mixed silicate-molybdate monolayer". The characteristic band of silanol groups is also strongly reduced in intensity. The IR spectrum of the activated pressed disk (Fig. 7) of MoA shows a sharp absorption at 1005 cm^{-1}, due to νMo=O stretching of surface anhydrous molybdenyl species (Busca, 2002; Hillerová et al., 1997), more evident in the MoA-A subtraction. The presence of νSi-O modes prevents the detection of νMo=O in the case of MoSA. The same spectra also show a weak absorption just below 2000 cm^{-1} (Fig. 7, up, left), due to the overtone of νMo=O. In the case of MoA, this band presents two superimposed components at 1995 and 1988 cm^{-1}. For MoSA the band is at 1995 cm^{-1} with a quite prominent component near 2005 cm^{-1}. For the position of the νMo=O, the stronger the ligands basicity, the lower νMo=O (Hillerová et al., 1997). Thus, part of the molybdenyl species in the case of MoA interacts with cation-anion centers of the alumina surface characterized by stronger acid-basicity. In contrast, on MoSA, more molybdenyl species interact with alumina sites characterized by lower acid-basicity.

3.3 CATALYST CHARACTERIZATION BY UV-VIS SPECTROSCOPY

The UV spectra of MoSA and MoA (Fig. 8) show strong absorptions associated to O^{2-} (2p) $\rightarrow$ Mo^{6+} (3d) charge transfer transitions (CTT). The UV-vis spectra recorded with the samples exposed to the ambient air and in dry atmosphere maintain the same features. Despite the same loading and nearly the same surface coverage (2.5-2.8 Mo at/nm^2support, almost corresponding to half of a monolayer (Ramirez, Cedeño, & Busca, 1999; Sankaranarayanan et al., 2011; Tian & Wachs, 2010), the two spectra, composed by two absorptions, differ very much in total intensity and in shape. Absorption (H), at 280 nm is much stronger in the spectrum of MoA than in MoSA,

while absorption (L), at 245 nm, is instead slightly stronger in the spectrum of MoSA than in that of MoA. Absorption (H) is attributed to species present in a relatively small amount but associated to a much higher extinction coefficient than absorption (L). Thus, the presence of silica in the support in some way limits the formation of species responsible for absorption (H), favoring the formation of species responsible for absorption (L).

Absorptions at $\lambda < 300$ nm are assigned essentially unanimously at present to "monomeric" tetrahedral molybdenyl species (Robertson, Gaudon, Jobic, Deniard, & Demourgues, 2011; Sankaranarayanan et al., 2011; Tian & Wachs, 2010), in agreement with the position of the main absorptions found for bulk compounds with tetrahedral molybdate structure (such as e.g. Na, Ca, Ba, Sr, Cd molybdates, β-$MgMoO_4$, α-$ZnMoO_4$ and $Al_2(MoO_4)_3$).

Polymeric molybdates (such as, e.g. anions of wolframite-type molybdates α-$CoMoO_4$ (Cavalcante et al., 2013) and β- $ZnMoO_4$ (Xiong et al., 1999) absorb at higher wavelength, i.e. $\lambda > 300$ nm as also iso-and hetero-polyoxomolybdates (Ramirez et al., 1999) do, which also have an overall coordination of six. The position of the main absorption of tetrahedral molybdates seems to depend on the Lewis acid strength of the cation involved. The (H) band is closely similar to that found for strongly bonded molybdates like $Al_2(MoO_4)_3$ (maximum at 270 nm), while the (L) band is similar to that of weakly perturbed $(MoO_4)^{2-}$ in water solution and in the case of Na_2MoO_4 (maximum near 230 nm, see (Ramirez et al., 1999).

Thus, we assign absorption (H) at 280 nm, which is reported to be present also on very low loading MoO_3-Al_2O_3 samples (Phung & Busca, 2015), to monomeric molybdate species bonded to the strongest cation-anion couple sites of the support, likely located on corners or edges of the alumina nanocrystals (Busca & Lorenzelli, 1982). The (L) band at 245 nm is assigned to weakly perturbed molybdate species. The presence of strongly bonded silicate species interacting with the strongest Lewis acid-base couples of the support would displace from these sites a large part of molybdate species forcing them to disperse on the main faces of alumina nanocrystals, where weaker molybdate/alumina interaction can occur, producing species (L).

3.4 FE-SEM CATALYST CHARACTERIZATION

FE-SEM analyses using back-scattered electrons (BSE) (in Fig. 9 the micrographs of typical particles of MoA and MoSA are shown) indicate that molybdate species disperse on MoA and MoSA, while not forming MoO_3 particles. Considering that molybdenum has a much larger backscattering coefficient due to its higher atomic number than the other elements present on the samples, bulk Mo oxide particles, if any, are expected to show a strong brightness. FE- SEM experiments do not show very bright particles with very high molybdenum concentrations, thus excluding the formation of separate molybdenum oxides particles, in agreement with XRD and IR and Raman skeletal data. Our samples show quite homogenous brightness in the particles, due to a dispersion of molybdenum over the support surfaces. However, the EDX analysis from FESEM images show that on MoA molybdenum species tend to cover the entire particles with quite homogeneous concentrations (Mo 5-20 wt%) while on MoSA Mo species seem to be less homogenously distributed with zones of higher Mo concentrations (30-40 wt%).

3.5 CATALYTIC ACTIVITY IN ETHANOL CONVERSION

The conversion and selectivity in the ethanol conversion in absence of oxygen are shown in Fig. 10. As previously reported (Garbarino, Travi, Pani, Carnasciali, & Busca, 2015), the catalytic activity in terms of ethanol conversion of pure alumina is significantly higher than the one observed for SA. Both catalysts produce mainly diethylether at low temperature and low conversion, and ethylene at high temperature and high conversion, without acetaldehyde production. Selectivity to other products is very small (~0.3 %) for A, but significant for SA where, at high temperature and conversion, they are ~4.5 %, due to higher hydrocarbons, formed only at high temperature. These data confirm the high dehydration activity of these catalysts without any evident dehydrogenation activity.

When oxygen is fed together with ethanol (Fig. 11, left), the conversion of ethanol on A is further increased, despite the lower concentration of ethanol in the feed. The selectivity towards diethyl ether and ethylene decreased because of the formation of several additional products,

such as acetaldehyde, ethylacetate, and C_4 hydrocarbons at partial conversion, CO and CO_2 at very high or full conversion. However, acetaldehyde yield never exceeds 20 %, and ethylene remains the principal product in while at full conversion (where CO and CO_2 are mostly produced). In these conditions oxygen conversion does not exceed 25 %, showing that the catalyst has very low oxidation activity. The low activity of pure alumina as an oxidation catalyst can be attributed to very small amounts of transition metal impurities (Finocchio et al., 1997). A similar behavior is found for SA (Fig. 11, right), which appears, however, to be less active than A in ethanol total oxidation at high temperature and less active in ethanol dehydration of diethylether, at low temperature, also in the presence of oxygen.

The same ethanol oxidation experiments have been performed over MoA and MoSA (Fig. 12). It is evident that molybdenum oxide promotes the conversion of oxygen and the formation of acetaldehyde, with high selectivity at high conversion. Yield to acetaldehyde is 74% at 573 K on MoA, with coproduction of some diethyl ether, ethylene, CO and CO_2. This corresponds to a strong decrease of the selectivity to diethyl ether at low conversion and of ethylene at high conversion. On the other hand, we found a decrease of ethanol conversion at low temperature on MoA with respect to A; this suggests that molybdenyl species, that certainly act as oxidation catalytic centers producing acetaldehyde, in parallel block the alumina's active sites for ethanol dehydration.

The effect of molybdenum addition on SA is a little different. In fact, in this case the conversion of ethanol is slightly increased at low temperature by the addition of molybdenum, producing acetaldehyde but also retaining significant activity in dehydration to diethyl ether. The selectivity and yield to acetaldehyde on MoSA is lower than on MoA, with residual activity in producing diethyl ether. At high temperature (above 623 K), the dehydration activity to ethylene is also definitely higher on MoSA than on MoA, while the oxidation activity (oxygen conversion, combustion activity) is lower on MoSA than on MoA.

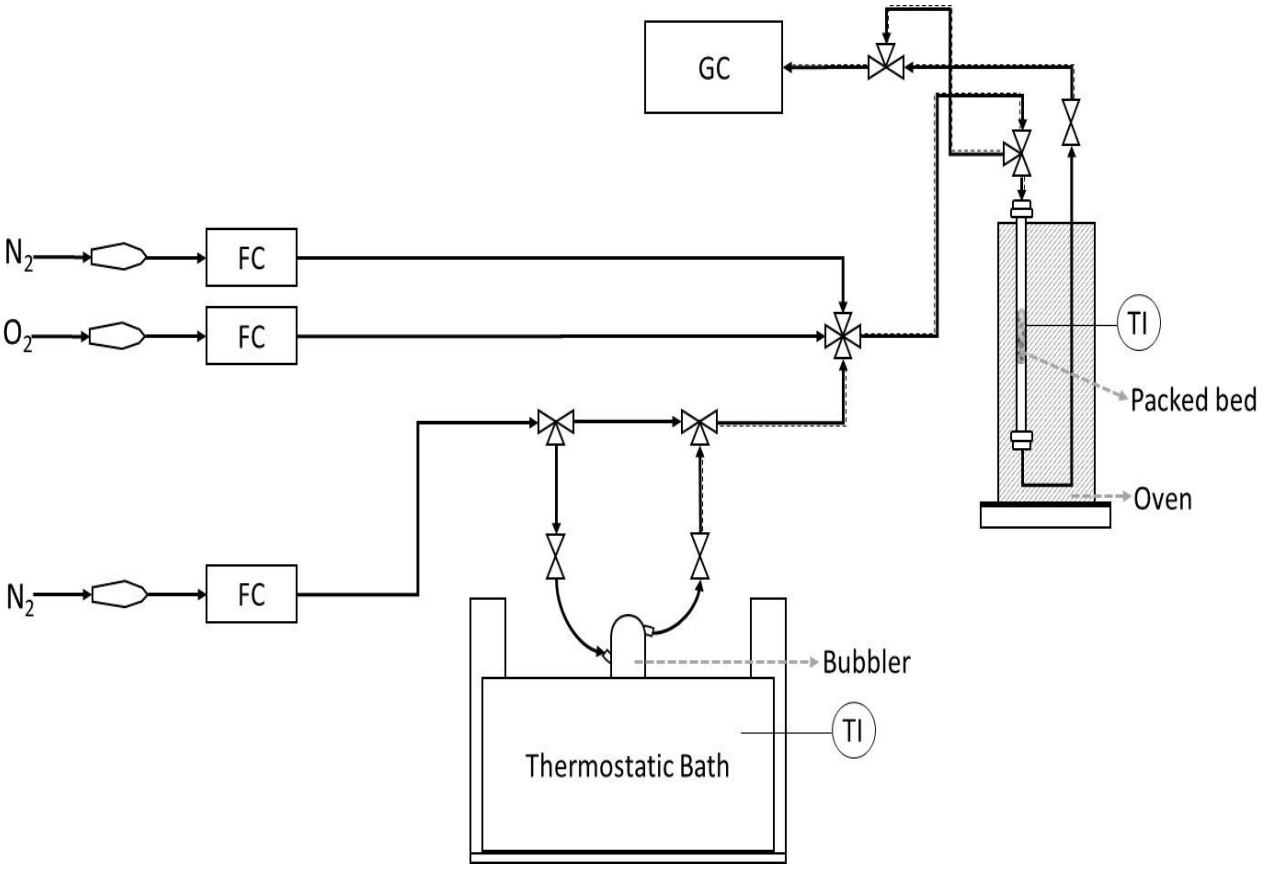

Fig. 1. Experimental set-up for testing catalytic performance.

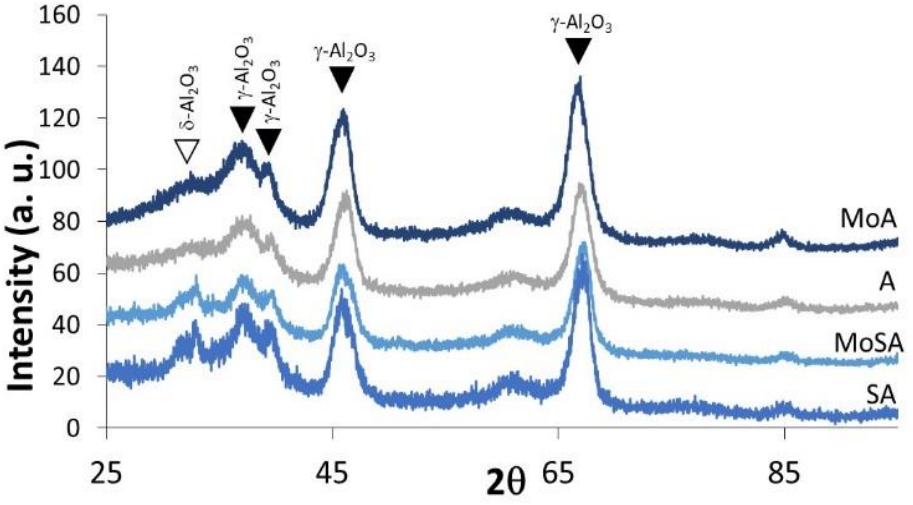

Fig. 2. X-ray diffraction of catalytic materials.

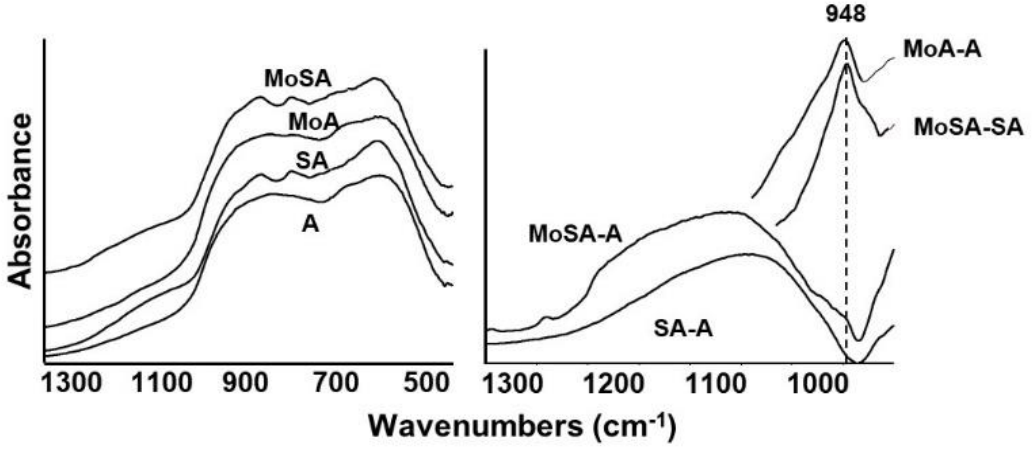

Fig. 3. Left: FT-IR skeletal spectra of supports and catalysts samples (KBr pressed disks). Right: subtraction spectra (Corresponding spectrum minus activated alumina surface).

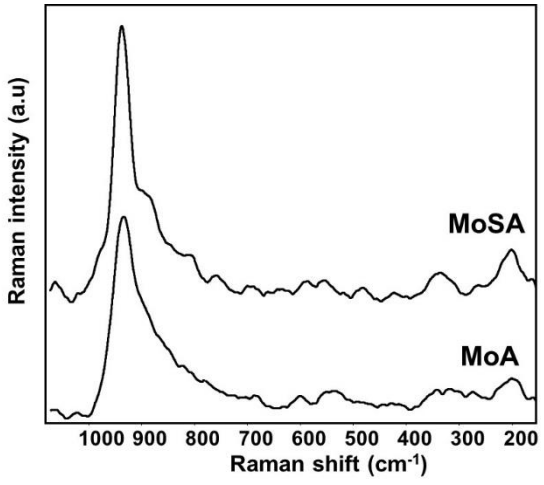

Fig. 4. Laser Raman spectra of Mo-containing samples (wet conditions).

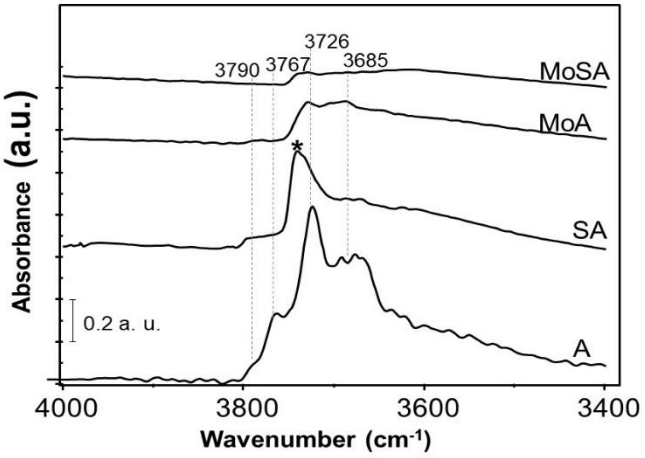

Fig. 5. FT-IR spectra in the OH stretching region of pure powder pressed disks, after activation in vacuum at 773 K for 1 h. * is indicating the band assigned to silanol groups.

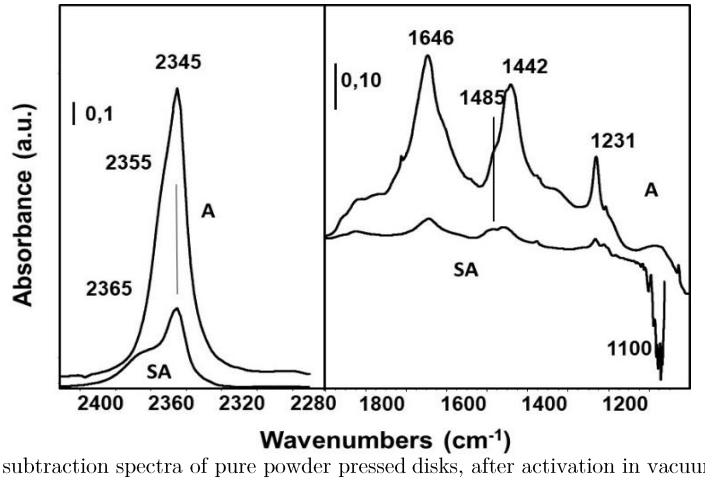

Fig. 6. FT-IR subtraction spectra of pure powder pressed disks, after activation in vacuum at 773 K 1 h and after contact with CO_2 (20 Torr), and further outgassing at r.t.

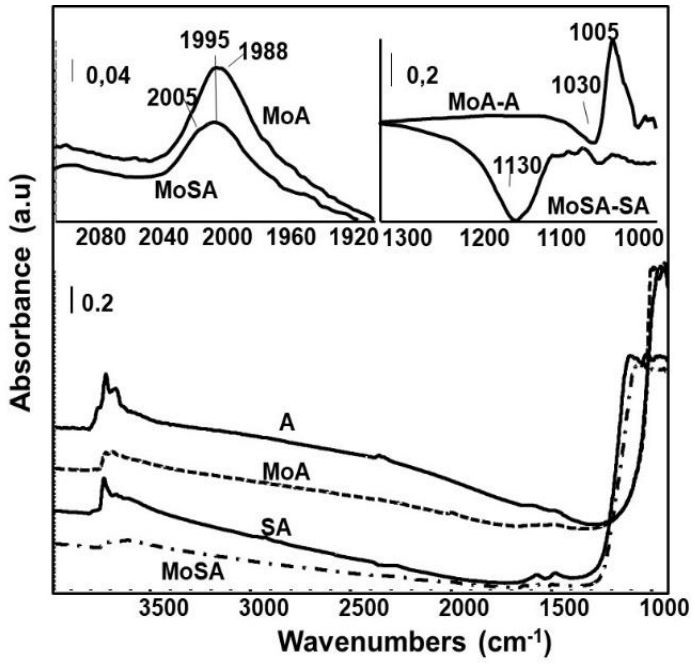

Fig. 7. Bottom: FT-IR spectra of pure powder pressed disks, after activation in vacuum at 773 K 1 h (full range). Top, left: region of overtones of Mo=O stretching vibrations. Top, right: subtractions.

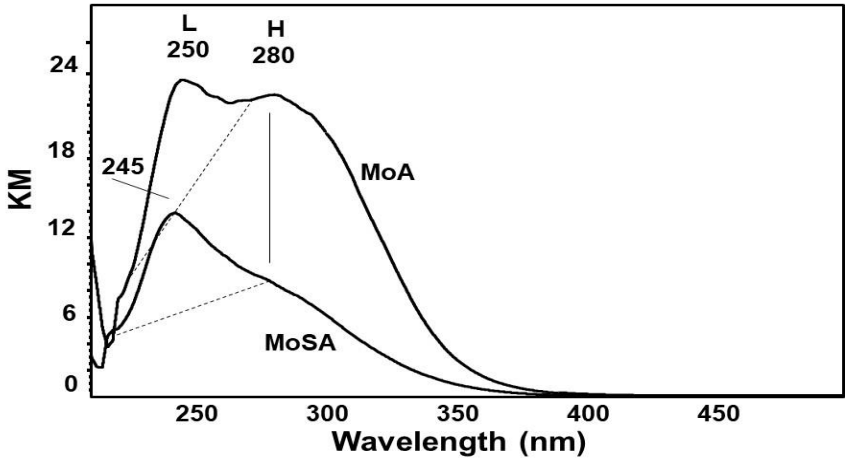

Fig. 8. Diffuse Reflectance UV-vis spectra of Mo-containing catalysts.

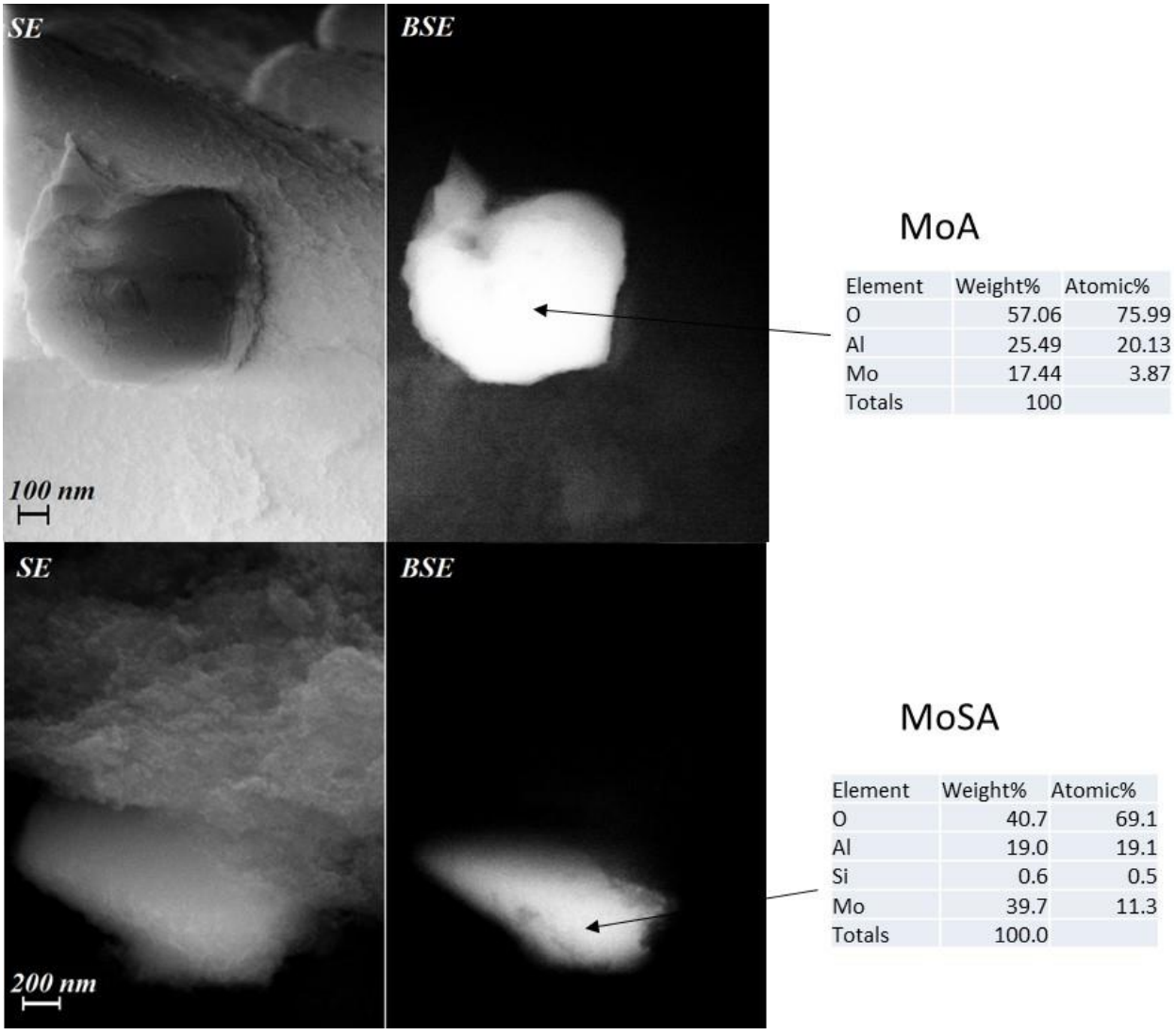

Fig. 9. FE-SEM micrographs acquired respectively with Inlens (SE) detector (left) and Solid-State Detector (BSE) (right) of two typical particles of MoA (top) and MoSA (bottom).

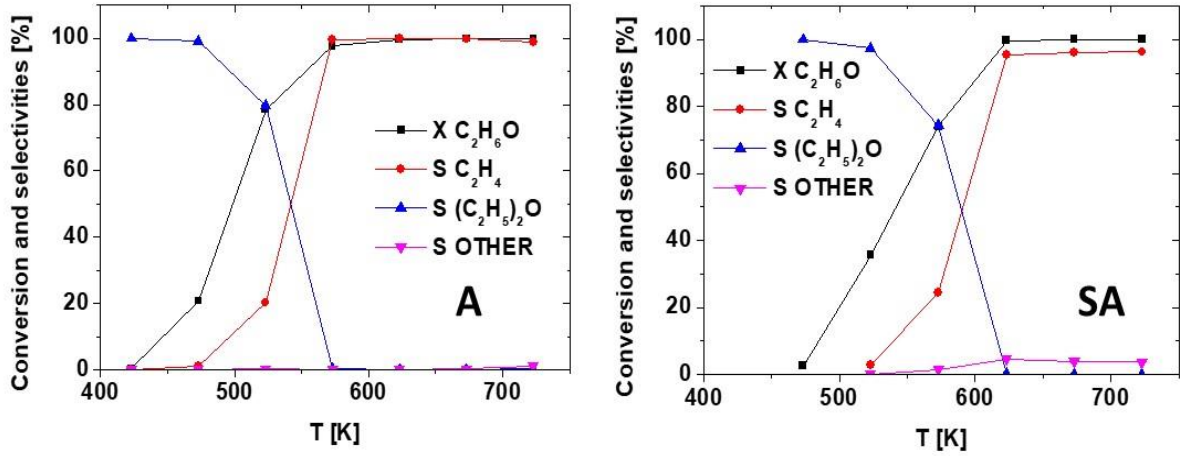

Fig. 10. Conversion and selectivity vs reaction temperature for the transformation of ethanol in the absence of oxygen over the alumina-based supports.

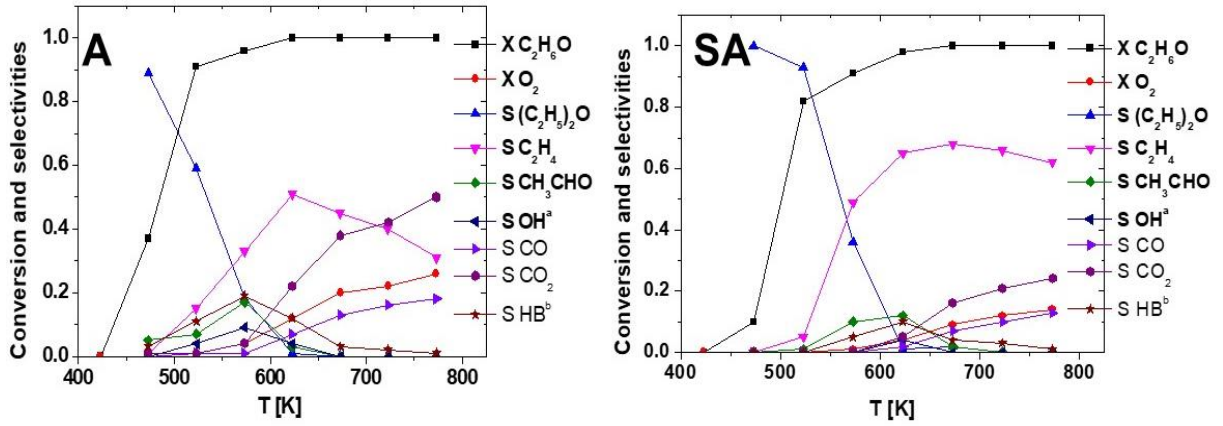

Fig. 11. Conversion and selectivity vs reaction temperature for the transformation of ethanol in the presence of oxygen over the alumina-based supports. OH^a= other oxygenates; HB^b= other hydrocarbons.

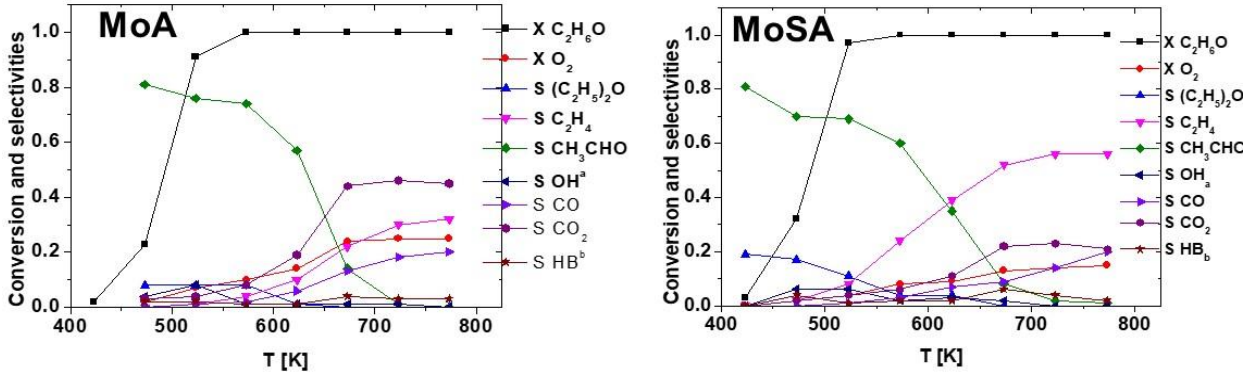

Fig. 12. Conversion and selectivity vs reaction temperature for the transformation of ethanol in the presence of oxygen for the molybdena catalysts. OH^a = other oxygenates; HB^b = other hydrocarbons.

4. DISCUSSION

The reactivity data and characterization results presented and discussed reveal a significant effect of the presence of a small amount of silica on alumina used as a support for preparing molybdena oxidation catalysts. The characterization data show that adding 5% silica strongly modifies the surface of alumina. In agreement with previous studies (Mouat et al., 2015; Zhang, Desikan, & Oyama, 1995), small amounts of silica disperse on the surface of alumina predominantly in the form of isolated hydrogen- orthosilicate species. Our results show that these silica species block specifically the alumina's acid-base sites, which are responsible for the adsorption of CO_2 in the form of hydrogencarbonate species, as well as with the strong decrease of the IR bands due to free surface OH's of alumina. These data support the idea that orthosilicate species anchor to specific alumina's sites, i.e. the strongest acid-base pairs, which are very likely located on edges, corners and surface defects of the alumina nanocrystals.

This behavior explains the lower catalytic activity in ethanol conversion of SA with respect to A, both producing diethyl ether at low conversion and temperature and ethylene at high conversion and temperature. A is more active than SA due to the stronger and higher amount of Lewis acid sites exposed on surface defects of the nanocrystals, part of which are "neutralized" by surface silicates. Also, in the presence of oxygen, A is more active in converting ethanol than SA, producing more oxidation products, suggesting that Lewis sites may also act as active sites for catalytic oxidation, although the presence of transition metal impurities may be a relevant factor in both cases.

The addition of molybdena to alumina introduces a high activity in oxidation catalysis, with the production of acetaldehyde with high yields in the temperature range 470-570 K. Our data agree with the few published data on the same system (Janlamool & Jongsomjit, 2015; Nair, Gatt, Miller, & Baertsch, 2011). The catalytic activity of our MoO_3/Al_2O_3 catalyst may be considered as interesting because of the remarkably high selectivity still obtained at nearly total conversion, thus allowing very high yields. In fact, in the case of the most active catalysts for this reaction, such as silver based (Dutov, Mamontov, Sobolev, & Vodyankina, 2016; Santacesaria, Sorrentino, Tesser, Di Serio, & Ruggiero, 2004) and supported vanadia catalysts (Hidalgo-Herrador, Tišler, Kubička, Raabova, & Bulanek, 2016; Setnička, Tišler, Kubička, & Bulánek, 2015), very high selectivity is obtained, but only at moderate or low conversion. Over the MoA catalyst, 74% yield to acetaldehyde is obtained at 573 K with total conversion, in part due to the very low production of diethyl ether, associated to the blocking of the alumina dehydration sites by molybdenyl species. The composition of the catalyst investigated here is similar to that reported in several studies to allow good yields also in other oxidation reactions such as paraffin oxidative dehydrogenations (Chen, Xie, Bell, & Iglesia, 2000; Sarrín et al., 1999). The performance in ethanol oxidative dehydrogenation could further be optimized by fine tuning of the molybdenum content as well as by doping with additional components.

The presence of silica on MoO_3/Al_2O_3 catalyst has an evident effect, reducing the selectivity both to acetaldehyde at low temperature and to COx at high temperature, while increasing (with respect to the silica-free catalyst) the selectivity to diethyl ether at low temperature and ethylene at high temperature. This provides evidence of a higher oxidation activity of molybdenum oxide centers of silica-free alumina than on silicated alumina. Indeed, the data show that in both cases molybdenum oxide centers are essentially dispersed, without any formation of molybdenum oxide particles, according to XRD, IR, Raman and FESEM. On the other hand, the EDX analyses from FESEM images indicates that dispersion is not uniform, with more concentrated Mo-based rafts on MoSA than on MoA. Additionally, UV spectroscopic data provide evidence of marked differences in the electronic structure of predominant molybdenum oxide species over the two supports.

The UV spectroscopy results agree with literature data on MoO_3/Al_2O_3 showing that low loading samples present isolated species with tetrahedral-like coordination (Tian & Wachs, 2010; Robertson et al., 2011), which are more hardly reducible (Sarrazin, Kasztelan, Payen, Bonnelle, & Grimblot, 1993; Sarrín et al., 1999), have lower acid strength (Goncharova, Boreskov, Yurieva, Yurchenko, & Boldyreva, 1981) and have lower activation energies for ethanol oxidation, and higher selectivity to acetaldehyde at low conversion (Nair et al., 2011) than medium Mo loading samples. These tetrahedral species are water insoluble, thus being more strongly bonded, in contrast to species present on higher Mo loading samples, which are water soluble [51]. The formation of these tetrahedral species, absorbing at $\lambda \sim 280$ nm, interacting with the strongest acid-base alumina sites, would be prevented by silicate species that displace molybdates towards weaker acid-base alumina sites, producing species (L) absorbing at $\lambda \sim 250$ nm. The Mo species formed on silica- containing alumina are characterized also by a slightly higher frequency component of the Mo=O stretching mode in dry conditions, in agreement with the lower acido-basicity of the surface alumina sites where they are located. The different environment of the molybdenyl species, for which spectroscopies provide a clear evidence, influences their catalytic activity, giving rise to a more active redox behavior on the more strongly bonded molybdenyls predominant on the MoA sample, and a less active redox behavior and likely more acidity on the less strongly bonded molybdenyls predominant on the MoSA sample. The difference found for the behavior and structure of molybdenyl species over pure and silica-containing alumina, which was also the object of previous studies (Robertson et al., 2011), can be associated to the different behavior in sulfidation of molybdena catalysts when used as hydrotreating catalyst precursors. It has in fact been reported, that molybdena supported on silica-containing alumina undergoes easier sulfidation and allows the preparation of more active Ni-Mo HDS catalysts in the transformation of 4,6-dimethyldibenzothiophene with respect to silica-free catalysts (Sánchez-Minero et al., 2009). This can be related to the weaker bond of molybdenyl species to alumina, when small amounts of silica block the stronger acid- base sites of alumina, thus displacing molybdenyl species towards weaker acid-base sites allowing easier sulfidation of the Mo species.

The addition of silica to alumina as support for molybdena was already reported to modify the methathesis activity, improving it (Cui et al., 2014). The results presented here find a good parallelism with the data reported for B-containing MoO_3-Al_2O_3 catalysts, showing that the addition of boron also leads to weakened interactions between Mo oxides and the surface of Al_2O_3 affecting the activity of Co-Mo sulfide hydrotreating catalysts (Usman, Takaki, Kubota, & Okamoto, 2005). Similar conclusions were also reported concerning the addition of small amounts of silica to the alumina support in the case of NiO/Al_2O_3 catalysts for steam reforming (Garbarino, Chitsazan, Phung, Riani, & Busca, 2015) and of K_2O- Cr_2O_3/Al_2O_3 catalysts for paraffin dehydrogenation (Bekmukhamedov, Mukhamed'yarova, Egorova, & Lamberov, 2016) showing in all cases that silica shifts the other supported species over sites where a lower interaction occurs with the alumina support. Thus, this is a main aspect concerning the surface chemistry of supported multicomponent catalytic materials used as catalysts or precursors of metallic and sulphide catalysts.

5. CONCLUSIONS

Molybdenum catalysts supported on alumina (~12 % wt. MoO_3) are interesting catalysts for the oxidative dehydrogenation of ethanol to acetaldehyde, giving rise to 74 % yield at 573 K, with high selectivity at nearly total conversion. The addition of small amounts of silica is detrimental for the catalyst performance for this reaction, reducing oxidation activity while increasing acid activity.

Two kinds of molybdenyl species form on the surface. Those interacting with the strongest alumina's acid-base couples (probably located on edges, corners and defects of the nanocrystals), are more active as oxidation catalytic centers, while those interacting with the weakest acid-base couples (probably located on plane faces), are more active as acid centers. The presence of silica on alumina prevent the molybdena species to anchor in the strongest alumina's acid-base couples and displaced them to weaker ones, where weaker metal-support interactions occur.

ACKNOWLEDGMENTS

We acknowledge CICY A.C. for the Raman facilities, FQ-UNAM-PAIP-5000-9072, and DGAPA-UNAM (PAPIIT-IN-113015) for financial support. AVM acknowled-ges scholarship from CONACyT, México (PhD grant 419865).

CONFLICT OF INTEREST

The authors have no conflicts of interest to declare.

REFERENCES

Akbari, A., Omidkhah, M., & Towfighi, D. (2014). Optimization of operating conditions in oxidation of dibenzothiophene in the light hydrocarbon model. *Chemical Industry and Chemical Engineering Quarterly*, *20*(3), 315–323. https://doi.org/10.2298/CICEQ121210013A

Balat, M. (2011). Production of bioethanol from lignocellulosic materials via the biochemical pathway: A review. *Energy Conversion and Management*, *52*(2), 858–875. https://doi.org/10.1016/J.ENCONMAN.2010.08.013

Bekmukhamedov, G., Mukhamed'yarova, A., Egorova, S., & Lamberov, A. (2016). *Modification by SiO_2 of Alumina Support for Light Alkane Dehydrogenation Catalysts. Catalysts* (Vol. 6). https://doi.org/10.3390/catal6100162

Busca, G. (2002). Differentiation of mono-oxo and polyoxo and of monomeric and polymeric vanadate, molybdate and tungstate species in metal oxide catalysts by IR and Raman spectroscopy. *Journal of Raman Spectroscopy*, *33*(5), 348–358. https://doi.org/10.1002/jrs.867

Busca, G. (2014). Structural, Surface, and Catalytic Properties of Aluminas. In *Advances in Catalysis* (pp. 319–404). https://doi.org/10.1016/B978-0-12-800127-1.00003-5

Busca, G., & Lavalley, J. C. (1986). Use of overtone bands to monitor the state of the catalyst active phases during infrared studies of adsorption and catalytic reactions. *Spectrochimica Acta Part A: Molecular Spectroscopy*, *42*(4), 443–445. https://doi.org/10.1016/05848539(86)80037-X

Busca, G., & Lorenzelli, V. (1982). Infrared Spectroscopic Identification of Species Arising From Reactive Adsorption of Carbon Oxides on Metal Oxide Surfaces. *Materials Chemistry*, *7*, 89–126.

Cavalcante, L. S., Moraes, E., Almeida, M., Dalmaschio, C., Batista, N. C., Varela, J., … & Beltrán, A. (2013). A combined theoretical and experimental study of electronic structure and optical properties of β-ZnMoO4 microcrystals. *Polyhedron*, *54*, 13–25.

Chauvel, A., & Lefebvre, G. (1989). *PETROCHEMICAL PROCESSES*. Editions Technip. Retrieved from https://books.google.com.mx/books?id=jH05AQAAIAAJ

Chen, K., Xie, S., Bell, A., & Iglesia, E. (2000). Structure and Properties of Oxidative Dehydrogenation Catalysts Based on MoO_3/Al_2O_3. *Journal of Catalysis - J CATAL*, *198*.

Cui, Y., Liu, N., Xia, Y., Lv, J., Zheng, S., Xue, N., … & Ding, W. (2014). *Efficient self-metathesis of 1-butene on molybdenum oxide supported on silica modified one-dimensional γ-Al_2O_3. Journal of Molecular Catalysis A:*

Chemical (Vol. 394). https://doi.org/10.1016/j.molcata.2014.06.027

Dutov, V. V., Mamontov, G. V., Sobolev, V. I., & Vodyankina, O. V. (2016). Silica-supported silver-containing OMS-2 catalysts for ethanol oxidative dehydrogenation. *Catalysis Today*, *278*, 164–173. https://doi.org/10.1016/j.cattod.2016.05.058

Eckert, M., Fleischmann, G., Jira, R., Hermann, M. B., & Golka, K. (2006). Acetaldehyde. In *Ullmann's Encyclopedia of Industrial Chemistry*. American Cancer Society. https://doi.org/10.1002/14356007.a01_031.pub2

Finocchio, E., Busca, G., Rossini, S., Cornaro, U., Piccoli, V., & Miglio, R. (1997). FT-IR characterization of silicated aluminas, active olefin skeletal isomerization catalysts. *Catalysis Today*, *33*(1), 335–352. https://doi.org/10.1016/S0920-5861(96)00106-X

Garbarino, G., Chitsazan, S., Phung, K., Riani, P., & Busca, G. (2015). *Preparation of supported catalysts: A study of the effect of small amounts of silica on Ni/Al₂O₃ catalysts. Applied Catalysis A: General* (Vol. 505). https://doi.org/10.1016/j.apcata.2015.07.017

Garbarino, G., Travi, I., Pani, M., Carnasciali, M., & Busca, G. (2015). Pure vs ultra-pure γ-alumina: A spectroscopic study and catalysis of ethanol conversion. *Catalysis Communications*, *70, 77-81. http://doi.org/10.1016/J.CATCOM.2015.07.016.*

Haddad, N., Bordes-Richard, E., Hilaire, L., & Barama, A. (2007). Oxidative dehydrogenation of ethane to ethene on alumina-supported molybdenum-based catalysts modified by vanadium and phosphorus. *Catalysis Today*, *126*(1), 256–263. https://doi.org/10.1016/j.cattod.2007.01.070

Hidalgo Herrador, J. M., Tišler, Z., Kubička, D., Raabova, K., & Bulanek, R. (2016). (V)/Hydrotalcite, (V)/Al_2O_3, (V)/TiO_2 and (V)/SBA-15 catalysts for the partial oxidation of ethanol to acetaldehyde. *Journal of Molecular Catalysis A: Chemical*, *420, 178-189.*

Hillerová, E., Morishige, H., Inamura, K., & Zdražil, M. (1997). Formation of monolayer of molybdena over alumina by unconventional slurry impregnation or solvent assisted spreading method. *Applied Catalysis A: General*, *156*(1), 1–17. https://doi.org/10.1016/S0926-860X(96)00406-1

Goncharova, O. I., Boreskov, G. K., Yurieva, T. M., Yurchenko, E. N., & Boldyreva, N. N. (1981). *Active state of molybdenum in molybdenum-alumina catalysts for propylene oxidation. Reaction Kinetics and Catalysis Letters* (Vol. 16). https://doi.org/10.1007/BF02066589

Janlamool, J., & Jongsomjit, B. (2015). Oxidative dehydrogenation of ethanol over AgLi-Al_2O_3 catalysts containing different phases of alumina. *Catalysis Communications*, *70*, 49–52. https://doi.org/10.1016/j.catcom.2015.07.020

Limayem, A., & Ricke, S. C. (2012). Lignocellulosic biomass for bioethanol production: Current perspectives, potential issues and future prospects. *Progress in Energy and Combustion Science*, *38*(4), 449–467. https://doi.org/10.1016/j.pecs.2012.03.002

Marakatti, V. S., Mumbaraddi, D., Shanbhag, G. V, Halgeri, A. B., & Maradur, S. P. (2015). Molybdenum oxide/[gamma]-alumina: an efficient solid acid catalyst for the synthesis of nopol by Prins reaction. *RSC Adv.*, *5*(113), 93452–93462. https://doi.org/10.1039/C5RA12106J

Mohsenzadeh, A., Zamani, A., & Taherzadeh, M. J. (2017). Bioethylene Production from Ethanol: A Review and Techno-economical Evaluation. *ChemBioEng Reviews*, *4*(2), 75–91. https://doi.org/10.1002/cben.201600025

Mouat, A. R., George, C., Kobayashi, T., Pruski, M., Van Duyne, R. P., Marks, T. J., & Stair, P. C. (2015). Highly Dispersed SiO_x/Al_2O_3 Catalysts Illuminate the Reactivity of Isolated Silanol Sites. *Angewandte Chemie - International Edition*, *54*(45), 13346–13351. https://doi.org/10.1002/anie.201505452

Nair, H., E. Gatt, J., Miller, J., & Baertsch, C. (2011). Mechanistic insights into the formation of acetaldehyde and diethyl ether from ethanol over supported VOx, MoOx, and WOx catalysts. *Journal of Catalysis*, *279*, 144–154.

Noureddini, H., & Kanabur, M. (1999). Liquid-Phase Catalytic Oxidation of Unsaturated Fatty Acids Liquid-Phase Catalytic Oxidation of Unsaturated Fatty Acids. *Journal of the American Oil Chemists' Society*, *76*(3), 305–311.

Peeters, I., van der Gon, A. W. D., Reijme, M. A., Kooyman, P. J., de Jong, A. M., van Grondelle, J., … van Santen, R. A. (1998). Structure–Activity Relationships in the Ammoxidation of Ethylene in the Absence of Molecular Oxygen over γ-Al_2O_3-Supported Molybdenum Oxide Catalysts. *Journal of Catalysis*, *173*(1), 28–42. https://doi.org/10.1006/jcat.1997.1879

Phung, K., & Busca, G. (2015). Ethanol dehydration on silica-aluminas: Active sites and ethylene / diethyl ether selectivities. *Catalysis Communications*, *68, 110-115.*

Phung, T. K., Proietti Hernández, L., Lagazzo, A., & Busca, G. (2015). Dehydration of ethanol over zeolites, silica alumina and alumina: Lewis acidity, Brønsted acidity and confinement effects. *Applied Catalysis A: General*, *493*, 77–89. https://doi.org/10.1016/j.apcata.2014.12.047

Ramirez, J., Cedeño, L., & Busca, G. (1999). The role of titania support in Mo-based hydrodesulfurization catalysts. *Journal of Catalysis*, *184*(1), 59–67. https://doi.org/10.1006/jcat.1999.2451

Ramirez, J., & Sánchez-Minero, F. (2008). *Support effects in the hydrotreatment of model molecules. Catalysis Today, 130.* https://doi.org/10.1016/j.cattod.2007.10.103

Robertson, L. C., Gaudon, M., Jobic, S., Deniard, P., & Demourgues, A. (2011). Investigation of the First-Order Phase Transition in the $Co_{1-x}Mg_xMoO_4$ Solid Solution

and Discussion of the Associated Thermochromic Behavior. *Inorganic Chemistry*, *50*(7), 2878–2884. https://doi.org/10.1021/ic102079f

Sánchez-Minero, F., Ramírez, J., Cuevas-García, R., Gutierrez-Alejandre, A., & Fernández-Vargas, C. (2009). *Kinetic study of the HDS of 4,6-DMDBT over NiMo/Al2O 3-SiO2(x) catalysts. Industrial & Engineering Chemistry Research - IND ENG CHEM RES* (Vol. 48). https://doi.org/10.1021/ie8005808

Sankaranarayanan, T. M., Pandurangan, A., Banu, M., & Sivasanker, S. (2011). Transesterification of sunflower oil over MoO_3 supported on alumina. *Applied Catalysis A: General*, *409–410*, 239–247. https://doi.org/10.1016/j.apcata.2011.10.013

Santacesaria, E., Sorrentino, A., Tesser, R., Di Serio, M., & Ruggiero, A. (2004). Oxidative dehydrogenation of ethanol to acetaldehyde on V_2O_5/TiO_2 - SiO_2 catalysts obtained by grafting vanadium and titanium alkoxides on silica. *J. Mol. Catal. A: Chem.*, *204*(1), 617–627. https://doi.org/10.1016/S1381-1169(03)00345-5

Sarrazin, P., Kasztelan, S., Payen, E., Bonnelle, J. P., & Grimblot, J. (1993). Interaction of oxomolybdenum species with .gamma.c-alumina and .gamma.c-alumina modified by silicon. 2. The molybdena/.gamma.c-alumina and molyb dena/silica/.gamma.c-alumina systems. *The Journal of Physical Chemistry*, *97*(22), 5954–5961. https://doi.org/10.1021/j100124a029

Sarrín, J., Noguera, O., Royo, H., Pérez Zurita, M. ., Scott, C., Goldwasser, M. ., … & Houalla, M. (1999). Effect of the preparation method on the reducibility of molybdena–alumina catalysts. *Journal of Molecular Catalysis A: Chemical*, *144*(3), 441–450. https://doi.org/10.1016/S1381-1169(99)00045-X

Setnička, M., Tišler, Z., Kubička, D., & Bulánek, R. (2015). Activity of Molybdenum Oxide Catalyst Supported on Al_2O_3, TiO_2, and SiO_2 Matrix in the Oxidative Dehydrogenation of n-Butane. *Topics in Catalysis*, *58*(14), 866–876. https://doi.org/10.1007/s11244-015-0453-2

Sheldon, R. A., & Van Bekkum, H. (2002). *Fine Chemicals through Heterogeneous Catalysis. Organic Process Research & Development* (Vol. 6). American Chemical Society. https://doi.org/10.1021/op020035e

Teimouri, A., Najari, B., Najafi Chermahini, A., Salavati, H., & Fazel-Najafabadi, M. (2014). Characterization and catalytic properties of molybdenum oxide catalysts supported on ZrO_2-γ-Al_2O_3 for ammoxidation of toluene. *RSC Adv.*, *4*(71), 37679–37686. https://doi.org/10.1039/C4RA07435A

Tian, H., Roberts, C.A., & Wachs, I. E. (2010). Molecular Structural Determination of Molybdena in Different Environments: Aqueous Solutions, Bulk Mixed Oxides, and Supported MoO_3 Catalysts. The Journal of Physical Chemistry C, 114, 14110-14120. https://doi.org/10.1021/jp103269w

Toulhoat, H., & Pascal. R. (2013). *Catalysis by transition metal sulfides: from molecular theory to industrial application*. (TECHNIP, Ed.) (1st ed.).

Usman, U., Takaki, M., Kubota, T., & Okamoto, Y. (2005). Effect of boron addition on a MoO_3/Al_2O_3 catalyst: Physicochemical characterization. *Applied Catalysis A: General* (Vol. 286). https://doi.org/10.1016/j.apcata.2005.03.020

Weissermel, K., & Arpe, H. J. (2003). *Industrial Organic Chemistry*. Wiley-VCH.

Xiong, G., Li, C., Feng, Z., Ying, P., Xin, Q., & Liu, J. (1999). Surface coordination structure of molybdate with extremely low loading on γ-alumina characterized by UV resonance Raman spectroscopy. *Journal of Catalysis*, *186*(1), 234–237. https://doi.org/10.1006/jcat.1999.2551

Zhang, W., Desikan, A., & Oyama, S. T. (1995). Effect of Support in Ethanol Oxidation on Molybdenum Oxide. *The Journal of Physical Chemistry*, *99*(39), 14468–14476. https://doi.org/10.1021/j100039a039